Quasi 1D Modeling of Mixed Compression Supersonic Inlets

George Kopasakis,[1] Joseph W. Connolly,[2] and Daniel E. Paxson[3]
NASA Glenn Research Center, Cleveland, Ohio 44135

Kyle J. Woolwine[4]
University of Florida, Gainesville, Florida 32611

The AeroServoElasticity task under the NASA Supersonics Project is developing dynamic models of the propulsion system and the vehicle in order to conduct research for integrated vehicle dynamic performance. As part of this effort, a nonlinear quasi 1-dimensional model of the 2-dimensional bifurcated mixed compression supersonic inlet is being developed. The model utilizes computational fluid dynamics for both the supersonic and subsonic diffusers. The oblique shocks are modeled utilizing compressible flow equations. This model also implements variable geometry required to control the normal shock position. The model is flexible and can also be utilized to simulate other mixed compression supersonic inlet designs. The model was validated both in time and in the frequency domain against the legacy LArge Perturbation INlet code, which has been previously verified using test data. This legacy code written in FORTRAN is quite extensive and complex in terms of the amount of software and number of subroutines. Further, the legacy code is not suitable for closed loop feedback controls design, and the simulation environment is not amenable to systems integration. Therefore, a solution is to develop an innovative, more simplified, mixed compression inlet model with the same steady state and dynamic performance as the legacy code that also can be used for controls design. The new nonlinear dynamic model is implemented in MATLAB Simulink. This environment allows easier development of linear models for controls design for shock positioning. The new model is also well suited for integration with a propulsion system model to study inlet/propulsion system performance, and integration with an aero-servo-elastic system model to study integrated vehicle ride quality, vehicle stability, and efficiency.

Nomenclature

A	=	area, m^2
a	=	local speed of sound, m/s
A_I	=	area of inlet opening at cowl lip, m^2
A_{IP}	=	area of inlet opening without centerbody at cowl lip, m^2
Cap	=	amount of shock captured by inlet
c_p	=	specific heat at constant pressure, J/(kg*K)
c_v	=	specific heat at constant volume, J/(kg*K)
F	=	flux term
H_t	=	total enthalpy, J/kg
M	=	Mach number
Mc	=	temporary Mach number
M_N	=	normal component of Mach number

[1]Senior Controls Engineer, Communications, Instrumentation and Controls Division, 21000 Brookpark Road, AIAA Member.
[2]Aerospace Engineer, Communications, Instrumentation and Controls Division, 21000 Brookpark Road, AIAA Senior Member
[3]Senior Aerospace Engineer, Communications, Instrumentation and Controls Division, 21000 Brookpark Road, AIAA Member.
[4]Student, non-member.

P = pressure, N/m^2
P_{TR} = total pressure ratio
R = universal gas constant, (N*m)/(kg*K)
S = source term
S_{12} = coefficient for artificial viscosity term
T = temperature, K
u_t = internal energy, J/kg
v = velocity, m/s
x = cell length, m
Y_{CB} = height of centerbody at cowl lip, m
Y_{CL} = height of cowl lip, m
Y_{SHK} = height of oblique shock at cowl lip, m
W = state term

Greek

β = shock angle, degrees
γ = ratio of specific heats
Δ = change in variable
θ = initial angle of centerbody, degrees
θ_L = angle of line connecting centerbody tip to cowl lip, degrees
ρ = density, kg/m^3

Subscripts

CL = state at cowl lip
j = conservation equation index
N = normal component
n = spatial index
s = static state
t = total state
∞ = free-stream condition

I. Introduction

IN a supersonic propulsion system the function of the inlet is to efficiently compress the incoming air to achieve high pressure recovery, before the air is delivered to the engine. For a mixed compression inlet, the air is first compressed through a series of external oblique shocks as shown in Fig. 1, followed by internal supersonic and subsonic compression. A normal shock is formed where the speed of the flow transitions through Mach 1, and the position of this shock is controlled near the inlet throat by utilizing bypass doors. The closer the shock position is controlled to the inlet throat the higher the inlet performance. However, the closer to the throat the shock is controlled the more unstable it becomes, which can cause the shock to be expelled. This can lead to inlet unstart, which is an undesirable condition. It is important to model the inlet dynamics in order to be able to design higher bandwidth controls with improved inlet performance for propulsion efficiency and for internal and external disturbance attenuation. Also, modeling the inlet dynamics is important for the purposes of developing integrated propulsion system models with improved control designs, integrated AeroPropusoServoElastic (APSE) models to assess couplings of the propulsion with the vehicle structural modes with associated performance issues such as vehicle stability and ride quality, and for integrated vehicle controls design studies.

Dynamic modeling for supersonic inlets has been covered before in several works. Primarily, inlet modeling for controls applications has originated from the discipline Computational Fluid Dynamics (CFD) based on discretization of the 3D and 2D Euler and Navier-Stokes equations.[1,2,3] These models have been reduced by developing an orthogonal basis to match selected frequency points or by singular value decomposition[4] to develop reduced order linear models. However, these laborious tasks are not necessary when the same objective can be accomplished starting with 1D CFD models. Secondly, it becomes a difficult process to design controls, if, for every change in inlet geometry, it becomes necessary to go back to 2D CFD codes. Lastly, it is desirable to start out with a more simplified nonlinear model that can also handle feedback controls and that runs with reasonable execution times. This allows inlet controls to be designed using linear models and validated against the nonlinear model at various operating conditions. It is assumed that the proof of a linear controls design would not be complete until it is

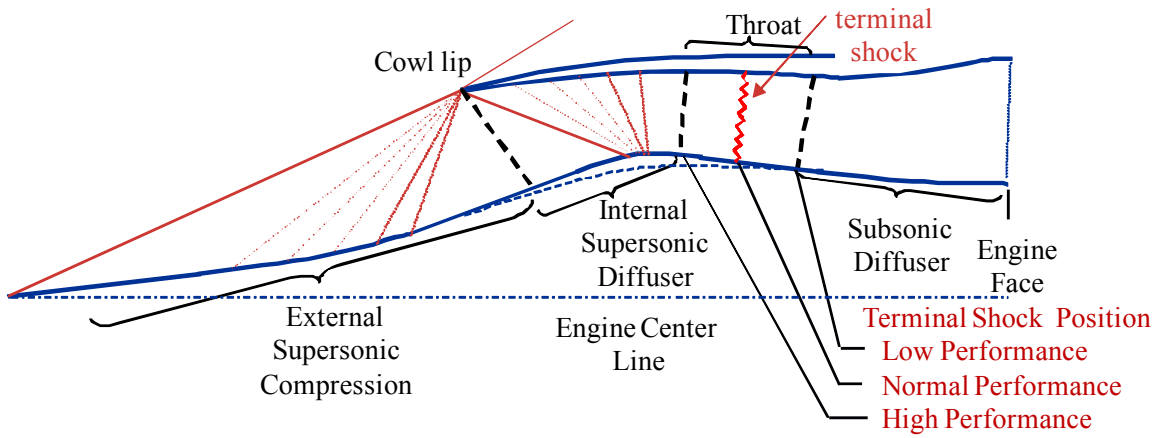

Figure 1. Center Line Diagram of a Mixed Compression Supersonic Inlet.

validated against the nonlinear inlet model, due to the increased sensitivity of the normal shock when its position is controlled near the throat area. Therefore, it is essential in this modeling effort that a quasi 1-D CFD mixed compression inlet model adequately captures the inlet dynamics for feedback control and for thrust dynamics.

The modeling approach presented in this paper is based on modeling the mixed compression inlet utilizing compressible flow equations together with quasi 1D CFD. A nonlinear inlet model named LAPIN[5] (LArge Perturbations INlet) based on the integration method of split characteristics was developed previously and implemented in FORTRAN. This model was not originally developed for controls design purposes and it cannot be used to continuously change the bypass air actuation system to control the normal shock. Also, LAPIN's code consists of about 80 FORTRAN program subroutines and because of relative poor documentation, reverse engineering of LAPIN to convert it to Simulink would be very time-consuming. The new model developed here utilizes a completely different technique to model the quasi 1D unsteady dynamics, which is considerably more simplified than the approach utilized in LAPIN, more intuitive and much easier to maintain. Therefore, this new model named NOIMA (NOnlinear Inlet Modeling Assembly), developed here for mixed compression inlets, is intended for use in place of LAPIN. The model is designed to be valid over the entire supersonic flight regime, with variations in altitude, Mach number, and associated variable inlet geometries. The inlet type selected for this development is the NASA 2-Dimensional Bifurcated (2DB) inlet design. However, the NOIMA modeling approach is generic and can be used to model any mixed compression inlet design. In LAPIN run time comparisons with NOIMA, it was also found that NOIMA runs approximately 3 times as fast. This new model, as was done with the rest of the propulsion system and the Aero-Servo-Elastic (ASE) simulation, is developed in MATLAB Simulink. This makes it more suitable for feedback controls design and integrated vehicle performance studies. However, LAPIN will still be used to validate NOIMA, since LAPIN was previously validated against experimental data.[5]

The model NOIMA has been developed using 1D CFD, utilizing central difference integration to solve the spatial derivatives. It assumes ideal gas with no frictional or viscous effects. However, artificial viscosity is implemented in this model to reduce shock oscillations and to generate a numerically stable solution. This model also accounts for the time derivatives of area variations due to actively changing the inlet geometry. Compressible flow relations are used to model external compression for the oblique shocks. The bleed and bypass system dynamics are not yet incorporated in this model version. It is assumed in this model that the external compressible flow dynamics are fast and are therefore neglected. Also, NOIMA has not been extended here to cover the conditions of inlet start and unstart. Even though NOIMA utilizes the 2DB inlet geometry to validate the modeling approach, the approach is generic and can be used to model any mixed compression inlet design by substituting the appropriate inlet geometry and boundary conditions.

The model NOIMA also complements an approach described in References 6, 7, and 8 for modeling engine components, towards developing an integrated propulsion system model. Thus this modeling effort, together with a separate effort to develop a vehicle AeroServoElastic (ASE) model, is part of an overall effort to develop an APSE vehicle model for performance studies, such as vehicle stability and ride quality.

This paper is organized as follows. First, the NOIMA inlet modeling approach is described for both external and internal supersonic and subsonic compression. This is followed by validation results of the NOIMA model utilizing LAPIN. Finally, some concluding remarks are offered.

II. Mixed Compression Inlet Model

In a mixed compression inlet, external supersonic compression is accomplished by the flow being compressed via a series of oblique shocks attached to the forward center body section of the inlet and extending to the cowl lip, as shown in Fig. 1. The centerbody geometry is adjustable, collapsing for a square type inlet and collapsing and retracting for an axisymmetric inlet. Normally, the centerbody geometry is set through a controls schedule to maximize inlet performance at certain operating conditions. After external compression, the flow entering the inlet undergoes supersonic and subsonic compression, before entering the engine. Controlling of the shock position in the subsonic diffuser is accomplished by utilizing high bandwidth by-pass doors. Controlling the by-pass doors to position the normal shock is not covered here, but more can be found on this topic in Reference 9.

External compression is modeled in NOIMA utilizing compressible flow relations for the oblique shocks, without dynamics, by assuming that the external inlet dynamics are significantly faster than those of the internal flow dynamics.

In NOIMA, as in LAPIN, the height of the center body is modeled for ten discrete positions, listing the x-y coordinates that describe the shape of the centerbody, with interpolation used between discrete positions. There is an actuator arm length in the model associated with each of the ten discrete centerbody positions. Adjusting the centerbody geometry changes the cross sectional area of every CFD cell in the model. If the length for the actuator arm is changing with time, then a cubic spline interpolation is used to compute the inlet cell areas. Internal inlet dynamics are modeled in NOIMA by utilizing Euler compressible and inviscid flow, quasi 1-D CFD, but with added artificial viscosity in order to handle numerics for the normal shock.

The various components of this inlet model are described in the sections that follow.

A. External Compression Model

There are two variations developed in NOIMA to model external compression. The first model variation allows for the formation of multiple oblique shocks as well as conditions that develop detached bow shocks. The second model variation simply computes a single equivalent oblique shock, resulting in the same flow compression properties at the cowl lip as those produced by the multiple oblique shock model. The multiple oblique shock model also serves as a tool to verify that the particular inlet geometry, for the designed operating condition, maximizes inlet performance. This requires that the oblique shocks are focused at the vicinity of the cowl lip for this operating condition. The single equivalent oblique shock model is a simplification of the former, which also simplifies user involvement of computing discrete oblique shock angles. However, the latter modeling approach assumes that the geometry has been adequately verified for the given operating condition. Both approaches are only valid for those conditions that produce focused oblique shocks in the vicinity of the cowl lip. The reason is that if the oblique shocks are not focused at the vicinity of the cowl lip, a significant amount of the flow could be leaking to the freestream, which NOIMA is not intended to capture.

1. Multiple Oblique Shocks Model

As mentioned earlier, the usefulness of the multiple oblique shocks model is that it is capable of verifying whether the centerbody geometry of a continuously changing curvature is meeting the design objectives of producing oblique shocks that terminate in the vicinity of the cowl lip for the designed operating conditions. If the oblique shocks do not terminate at the vicinity of the cowl lip, this model (at present) becomes less accurate because it doesn't account for adjustments to flow field conditions due to flow spillage over the cowl lip. This model is also capable of discriminating for the conditions that generate undesirable bow shocks.

To develop this model or to apply this modeling approach to a different inlet geometry, the user is required to determine a series of discrete angle variations (one for each oblique shock) in order to approximate the continuous centerbody contours in a piecewise linear fashion. The angular variation of the centerbody contour is successively approximated, and by applying the compressible flow relations, that will be covered shortly, a series of oblique shocks are formed. This process is terminated before the first shock enters the supersonic diffuser. The granularity of approximating the centerbody contour varies along its length depending on the change of its geometry. This process is terminated when the entry Mach number at the cowl lip varies less than some predetermined quantity. In this process of discretizing the centerbody geometry, it is expected that for a working inlet geometry, at the designed supersonic cruise condition, all the oblique shocks will meet at the cowl lip. Also, for a translating or for a collapsing centerbody geometry, the centerbody needs to be placed at its appropriate predetermined position corresponding to that operating condition prior to determining the centerbody piecewise-linear geometry. However, this process of accurately determining the discrete centerbody angles can also vary depending on the operating condition.

Using the continuity equation and the fact that the tangential component of the flow velocity does not change across the shock, trigonometric relations[10] eventually lead to the following relation

$$\tan\theta = 2\cot\beta \frac{M_{1N}^2 - 1}{M_1^2(\gamma + \cos 2\beta) + 2} \tag{1}$$

where β and θ and γ in Eq. (1) are the shock angle, the initial angle of the centerbody, and the ratio of specific heats respectively, and M_{1N} is the normal component of the upstream Mach number (the subscript N stands for the normal component), defined as

$$M_{1N} = M_1 \sin\beta \tag{2}$$

Equation (1) can be solved for the shock angle β using a root finding method, knowing the flow Mach number M_1 before the shock and the local centerbody angle θ. For the first oblique shock, M_1 will be the freestream Mach number and θ will be the angle of the centerbody with respect to the freestream flow velocity. For subsequent oblique shocks, the angle θ will be the discrete change in angle, $\Delta\theta$, in a piece-wise linear fashion.

The rise in the static quantities of pressure P_2, density ρ_2, and temperature T_2 after the shock can be determined from the following relations

$$\frac{P_2}{P_1} = 1 + \frac{2\gamma}{\gamma + 1}\left(M_{1N}^2 - 1\right) \tag{3}$$

$$\frac{\rho_2}{\rho_1} = \frac{(\gamma + 1)M_{1N}^2}{(\gamma - 1)M_{1N}^2 - 2} \tag{4}$$

$$\frac{T_2}{T_1} = \frac{P_2}{P_1}\frac{\rho_1}{\rho_2} \tag{5}$$

The Mach number after the shock, M_2, is solved as

$$M_2 = \frac{1}{\sin(\beta - \theta)}\sqrt{\frac{1 + \frac{\gamma - 1}{2}M_{1N}^2}{\gamma M_{1N}^2 - \frac{\gamma - 1}{2}}} \tag{6}$$

For a given Mach number, M_1, a maximum angle, θ_{max}, exists beyond which the oblique shock will no longer be attached and is replaced by a detached bow shock. Therefore, additional code is incorporated in the model to cover conditions that give rise to bow shocks. Various references including Reference 10 include θ–β–M charts that show the transition from oblique to bow shocks.

2. Single Equivalent Oblique Shock Model

The single equivalent oblique shock model variation is based on the one used in the LAPIN code. For the supersonic cruise condition, it is found that the single shock model produces the same flow conditions as the multiple oblique shock model at the inlet entrance.

The oblique shock angle in this model is also computed using Eq. (1), with M_1 being the freestream Mach number. In this case, for the single equivalent oblique shock model, the centerbody angle, θ, pertains to the initial fixed body angle (where the centerbody wedge first meets the freestream) with respect to freestream flow velocity direction.

The total pressure ratio at the cowl lip can be computed as

$$\frac{P_{t,CL}}{P_{t,\infty}} = \left(\frac{\gamma+1}{2\gamma M_{1N}^2 - (\gamma-1)} \right)^{\frac{1}{\gamma-1}} \left(\frac{(\gamma+1)M_{1N}^2}{2+(\gamma+1)M_{1N}^2} \right)^{\frac{\gamma}{\gamma-1}} \tag{7}$$

If the shock angle, θ, calculated using Eq. (1), falls within the cowl lip, then the total pressure at the cowl lip is recalculated as

$$P_{TR} = \frac{\left(Y_{CL} - Y_{SHK}\right) + \frac{P_{t,CL}}{P_{t,\infty}}\left(Y_{SHK} - Y_{CB}\right)}{Y_{CL} - Y_{CB}} \tag{8}$$

where Y pertains to height from the centerbody centerline to the cowl lip (Y_{CL}), to the oblique shock at the cowl lip (Y_{SHK}), and to the centerbody at the cowl lip (Y_{CB}). For subsequent calculations, a variable C_{ap} (amount of shock captured by the inlet) is calculated, which is set to 1 for this case.

If the oblique shock does not get captured by the cowl lip, then total pressure ratio (P_{TR}) remains as that calculated by Eq. (7)

$$P_{TR} = \frac{P_{t,CL}}{P_{t,\infty}} \tag{9}$$

and C_{ap} is calculated as

$$C_{ap} = \frac{\frac{1}{\tan\theta} - \frac{1}{\tan\theta_L}}{\frac{1}{\tan\theta} - \frac{1}{\tan\beta}} \tag{10}$$

where θ_L is the angle of the line connecting the centerbody tip to the cowl lip with respect to the freestream flow velocity.

Then the Mach number, M_2, after the oblique shock, or in this case the Mach number at the cowl lip, M_{CL}, can be expressed as

$$M_{CL} - \sqrt{\left(\frac{2}{\gamma-1}\right)\left[\left(\frac{M_{CL}}{M_C}\right)^{\frac{2(\gamma-1)}{\gamma+1}} - 1\right]} = 0 \tag{11}$$

where M_C signifies a temporary Mach number, calculated as

$$M_C = \frac{M_\infty C_{ap} A_I}{\left(1 + \frac{(\gamma-1)}{2} M_\infty^2\right)^{\frac{\gamma+1}{2(\gamma-1)}} A_{IP} P_{TR}} \tag{12}$$

with A_I and A_{IP} signifying the area of inlet opening at the cowl lip and the area of inlet opening at the cowl lip without the presence of the centerbody, respectively. The Mach number, M_{CL}, in Eq. (11) can be calculated using a root finding method.

The static pressure and temperature at the cowl lip can be determined using compressible flow equations as

$$P_{s,CL} = P_{s,\infty} P_{TR} \left(\frac{1 + \frac{\gamma - 1}{2} M_{\infty}^2}{1 + \frac{\gamma - 1}{2} M_{CL}^2} \right)^{\frac{\gamma}{\gamma - 1}} \tag{13}$$

$$T_{s,CL} = T_{s,\infty} \left(\frac{1 + \frac{\gamma - 1}{2} M_{\infty}^2}{1 + \frac{\gamma - 1}{2} M_{CL}^2} \right) \tag{14}$$

For the case where the oblique shock does not get captured by the cowl lip, these formulations account for adjustments to flow conditions due to flow spillage over the cowl lip. Utilizing the single equivalent oblique shock model, the assumption is that at a given operating condition, the variable centerbody geometry is such that it produces oblique shocks that intersect at a focal point (whether above or below the cowl lip height). This assumption can be verified by using the multiple oblique shock model. In addition, care must be exercised to recognize conditions that generate bow shocks (i.e., referring to θ–β–M charts if necessary), since this model version is not designed to capture these conditions.

B. Internal Compression Model

The internal compression model consists of the supersonic internal compression portion and the subsonic compression portion. One-dimensional volume dynamics,[6] utilizing conservation equations, assuming ideal gas, with no frictional losses would be the easiest way to model the dynamics of mixed compression supersonic inlets. However, since communication in supersonic flow regimes only occurs in the downstream direction, this would not allow for shock movement in the upstream direction. On the other hand, CFD integration techniques employ averaging, like central differencing. This feature allows communication in the upstream direction for supersonic flow. Even though communication only occurs in the downstream direction for supersonic flow, the averaging technique in CFD that takes information from the upstream cells is physically realistic since it preserves continuity in the flow. Thus, it becomes apparent that CFD needs to be utilized to model the 1D flow dynamics of mixed compression inlets.

With the assumptions made above, the gas dynamics associated by applying continuity of mass, momentum, and energy to a flow are as follows.

$$\frac{\partial}{\partial t}(\rho_s A) + \frac{\partial}{\partial x}(\rho_s A v) = 0 \tag{15}$$

$$\frac{\partial}{\partial t}(\rho_s A v) + \frac{\partial}{\partial x}(\rho_s A v^2) = -A \frac{\partial P_s}{\partial x} \tag{16}$$

$$\frac{\partial}{\partial t}(\rho_s A E t) + \frac{\partial}{\partial x}(\rho_s A v H_t) = -P_s \frac{\partial A}{\partial t} \tag{17}$$

The conservation Eqs. (15) to (17) can be expressed in terms of the following general formulation as

$$\frac{\partial}{\partial t}(W_j) = -\frac{1}{A} \frac{\partial}{\partial x}(A F_j) + \frac{S_j}{A} \tag{18}$$

using the process described below.

Since the area of a supersonic inlet can change with time by manipulating its geometry, first it is necessary to take the partial derivatives in Eqs. (15) to (17) with respect to area and then reformulate these equations in terms of Eq. (18). By performing these manipulations (see Appendix 1 for detailed derivations), Eqs. (15) to (18) can be expressed as follows

$$\frac{\partial \rho_s}{\partial t} = -\frac{1}{A}\frac{\partial(\rho_s A v)}{\partial x} - \frac{\rho_s}{A}\frac{\partial A}{\partial t} \tag{19}$$

$$\frac{\partial}{\partial t}(\rho_s v) = -\frac{1}{A}\frac{\partial}{\partial x}\left[(P_s + \rho_s v^2)A\right] + \frac{1}{A}\left(P_s\frac{\partial A}{\partial x} - \rho_s v\frac{\partial A}{\partial t}\right) \tag{20}$$

$$\frac{\partial}{\partial t}\left[\left(\frac{P_s}{\gamma - 1} + \frac{\rho_s v^2}{2}\right)\right] = -\frac{1}{A}\frac{\partial}{\partial x}\left[A\left(\frac{\gamma P_s v}{\gamma - 1} + \frac{\rho_s v^3}{2}\right)\right] - \frac{1}{A}\left(\frac{\gamma P_s}{\gamma - 1} + \frac{\rho_s v^2}{2}\right)\frac{\partial A}{\partial t} \tag{21}$$

Equations (19) to (21) fit the general form of Eq. (18) with the equation terms given in Table 1.

Table 1. Equation (18) Terms.

j	*Wj*	*Fj*	*Sj*
1	ρ_s	$\rho_s v$	$-\rho_s\frac{\partial A}{\partial t}$
2	$\rho_s v$	$P_s + \rho_s v^2$	$P_s\frac{\partial A}{\partial x} - \rho_s v\frac{\partial A}{\partial t}$
3	$\frac{P_s}{\gamma - 1} + \frac{\rho_s v^2}{2}$	$\frac{\gamma P_s v}{\gamma - 1} + \frac{\rho_s v^3}{2}$	$-\left(\frac{\gamma P_s}{\gamma - 1} + \frac{\rho_s v^2}{2}\right)\frac{\partial A}{\partial t}$

Therefore Eq. (18) with the terms *Wj*, *Fj*, and *Sj*, respectively identifiable as the state, the flux, and the source terms, represents the model utilized for the individual cells of the quasi 1-D mixed compression inlet.

A central difference approach[11] is applied to Eq. (18) to approximate the spatial derivatives, and an artificial viscosity term is added for numerical stability to damp non-physical flow oscillations. This results in the following equation

$$\begin{aligned}\frac{\partial}{\partial t}(W_{j,n}) = &-\left(\frac{A_{n+1}F_{j,n+1} - A_{n-1}F_{j,n-1}}{2\Delta x A_n}\right) + \frac{S_{j,n}}{A_n} \\ &+ S_v\left[\frac{(|v_n| + a_n)(A_{n+1}W_{j,n+1} - A_n W_{j,n}) - (|v_{n-1}| + a_{n-1})(A_n W_{j,n} - A_{n-1}W_{j,n-1})}{\Delta x A_n}\right]\end{aligned} \tag{22}$$

The artificial viscosity coefficient, S_v, is a constant (0.05 in this case) and is chosen such that the normal shock numerical oscillations are reasonably damped, but not too damped because this will cause the shock to be smeared over the length of several cells.

Equation (22), covering the conservation equations, is used to model both internal supersonic and subsonic compression.

C. Boundary Conditions

Boundary conditions are necessary to run the inlet model. The first and the last cell of the inlet model without dynamics are constructed as ghost calls (i.e., non-physical cells) in order to establish boundary conditions. The upstream boundary condition at the cowl lip can also be satisfied by the external compression equations and the free-stream conditions. The downstream boundary condition that simulates the engine face can be fixed by either specifying the back pressure or the exit Mach number. For both of these cases the following characteristic equation can be used to compute the remainder of the exit states W_j.

$$\left(\frac{2}{\gamma-1}\right)a_{n-1}+v_{n-1}=\left(\frac{2}{\gamma-1}\right)a_n+v_n \tag{23}$$

Specifying a fixed mass flow rate for a boundary condition, which is necessary to tie the inlet to the rest of the engine model,[6] is not possible. The reason is that the solution for this case is non-deterministic and the simulation becomes unstable. This is due to the relation $\dot{W}=\rho Av$, which implies that for a fixed area, the density and velocity can vary freely as long as the specified fixed mass flow rate boundary condition is satisfied. However, this problem can be mitigated when the actual engine model is integrated with the inlet model. The reason is that given a mass flow rate and the core speed, calculated internally, for the compressor or the fan (whichever of the two interfaces the inlet), a fixed pressure ratio results via the component characteristics map. Thus, even though the mass flow rate is an input to upstream components for the engine simulation, the fan or compressor characteristics act as a ghost volume to fix the pressure for a given mass flow rate and speed between time steps. In terms of implementation for the integrated inlet/engine simulation, this boundary volume can also be implemented as a dynamic cell of a constant area mixing volume, modeled based on volume dynamics.[6] The inputs of this boundary volume are the mass flow rate coming from the engine and the states W_j coming from the inlet, with outputs of total temperature and total pressure going to the engine and the calculated W_j states of this volume going back to the n^{th} inlet cell.

III. Inlet Simulation Results

This section covers simulation results, both steady state and dynamic, with the objective of verifying the quasi 1D mixed compression inlet model NOIMA.

In the simulation, the CFD cell length, Δx, is kept constant for all the inlet cells. This is important to maintain the second order accuracy advantage of the central difference method. Using a variable Δx would require a complete reformulation of the conservation equations.

A. External Compression Results

A simulation of external compression is shown in Fig. 2. This simulation shows actual dimensions of the 2-Dimensional Bifurcated (2DB) inlet geometry, with the centerbody geometry shape depicting the supersonic cruise condition. The multiple shock angles shown are actual shock angles and corresponding Mach numbers calculated utilizing the multiple shock model. The discretization utilized for the variation in the centerbody angle, θ, that creates these multiple shocks, produces a difference of inlet flow conditions at the cowl lip significantly less than 1% compared to LAPIN results. Interestingly, these shock angles terminate at the vicinity of the cowl lip for the centerbody shape at cruise and for the cruise freestream conditions. This verifies that the actual 2DB inlet geometry is designed to maximize propulsion efficiency at the supersonic cruise condition.

Figure 3 shows the same inlet simulation utilizing the single shock model. The importance of Figs. 2 and 3 is that in this case both models predict the same Mach number at the cowl lip and the same flow conditions, which are utilized by the quasi 1-D CFD model that will be discussed later. Fig. 3 also shows the internal compression model results for the Mach number, which will be discussed in the next section. The bottom portion of this figure shows the Mach variation using a color scale. This single oblique shock model also produces differences significantly less than 1% for the flow conditions at the cowl lip compared to LAPIN. The user has the option to use either model, based on the qualifications already described.

B. Internal Compression Results

The steady state comparison with LAPIN for the internal portion of the inlet was performed at cruise freestream conditions and at a back pressure of 60,637 Pa, which represents engine face pressure for cruise operation. The LAPIN inlet exit area had an abrupt change for the last cell to apparently match it to the engine face. This area was smoothed out for NOIMA to make the simulation better behaved. This change caused an equivalent exit pressure change of 1%. Therefore, the exit boundary pressure for NOIMA was also increased by 1%. The centerbody position was held constant, with the actuator arm almost fully extended (i.e., near maximum centerbody height).

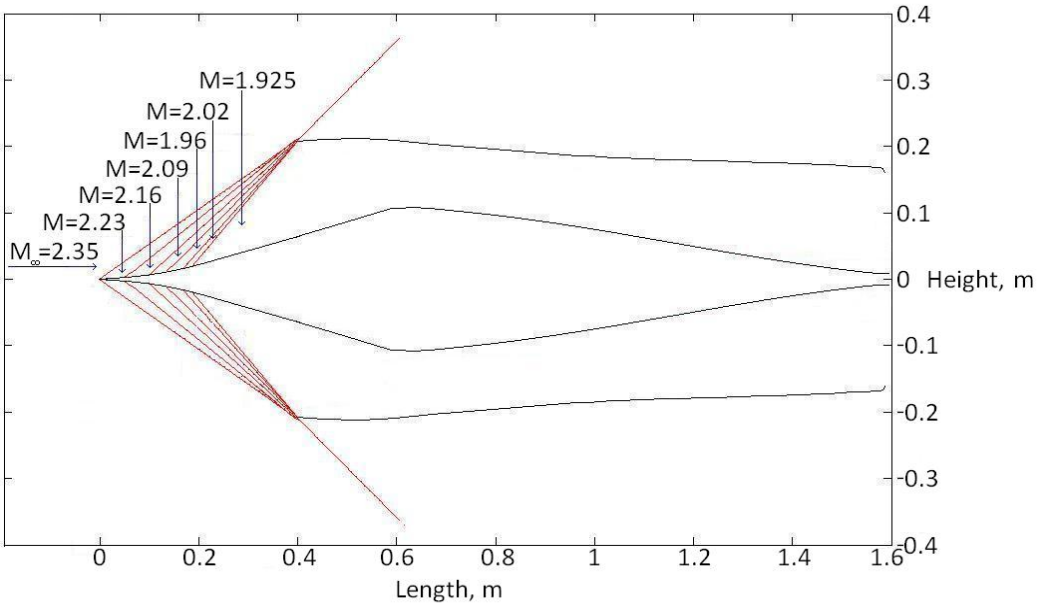

Figure 2. External Compression Utilizing Multiple Shock Model.

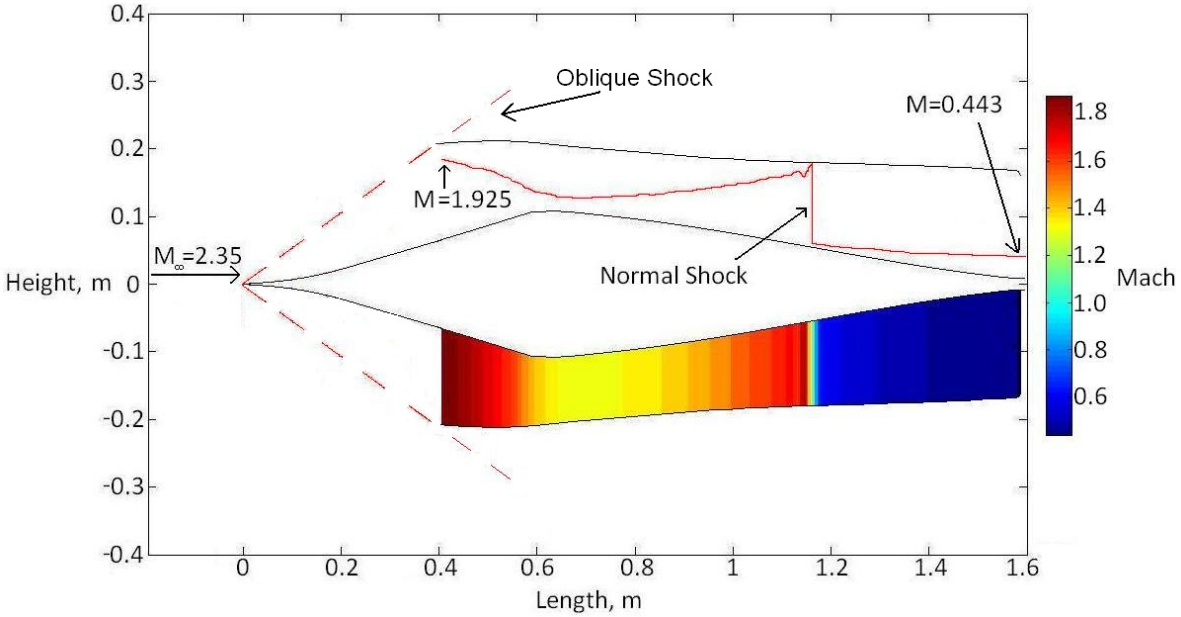

Figure 3. Mach number Profile for Integrated Inlet, Utilizing Single Oblique Shock External Compression Model.

In NOIMA, the inlet internal compression is simulated with a total of 133 cells, the same as LAPIN. The integrated inlet simulation results showed steady state differences of less than 1% for all the pressures, temperatures, and densities throughout the internal compression portions of the inlet. For the shock position, the difference was somewhat larger than 1%. Figure 4 shows a simulation of normalized pressure (normalized by the throat pressure) compared to LAPIN with the normalized inlet area (normalized by the throat area) across the length of the inlet. Figure 5 shows comparisons for normalized temperature (normalized by the throat temperature) and Figure 6 shows comparisons for the Mach number.

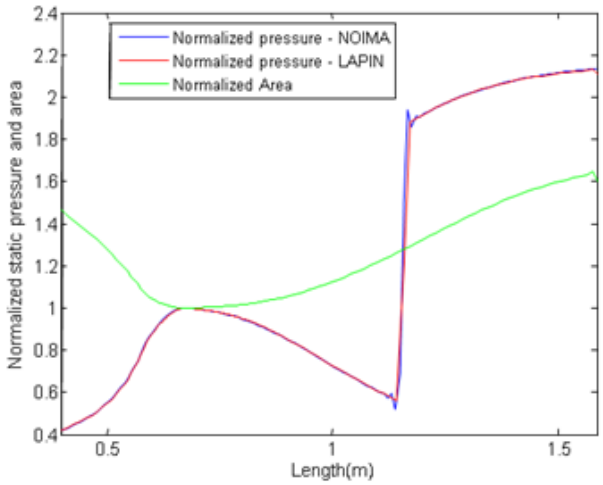

Figure 4. Steady State Inlet Static Pressure Ratio and Normalized Area.

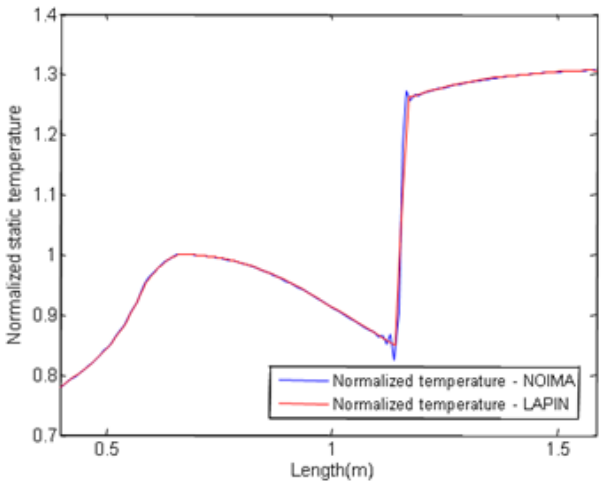

Figure 5. Steady State Inlet Static Temperature Ratio.

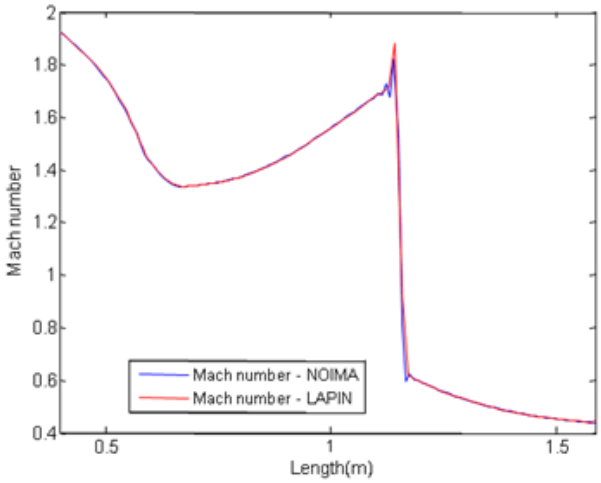

Figure 6. Steady State Inlet Mach Number.

A necessary feature of mixed compression inlets is the ability to alter the centerbody shape in order to maintain high performance at different operating conditions. Figure 7 shows a comparison of NOIMA results between the prior centerbody position, as shown in Fig. 4, and a simulation where the centerbody shape was changed by reducing the actuator arm extension by approximately 50% of its travel range. This figure shows the different static pressure profile throughout the inlet, with the shock moving closer to the throat position. It also shows the higher pressure recovery with this centerbody shape and with the shock positioned closer to the inlet throat.

Raising the back pressure will cause the shock to move upstream, towards the inlet throat. As the shock moves closer to the throat the rate at which it moves increases. This makes it more challenging for a control system to maintain the shock position near the throat for various internal and external flow disturbances. This behavior of the shock is illustrated in Fig. 8. In this test the back pressure was increased at a rate of 5% per second. The figure demonstrates the sensitivity of the shock position with respect to time. As it can be seen, the shock moves faster as it approaches the throat for the same amount of change in back pressure. Closer to the throat, the shock moves relatively rapidly (but not instantaneously), being expelled out of the inlet. The constant position shown right at the

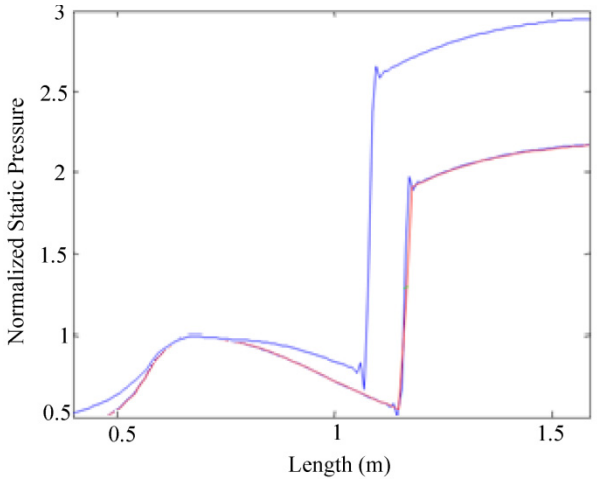

Figure 7. Steady State Inlet Static Pressure with Changed Centerbody Geometry (red unchanged, blue 50% change).

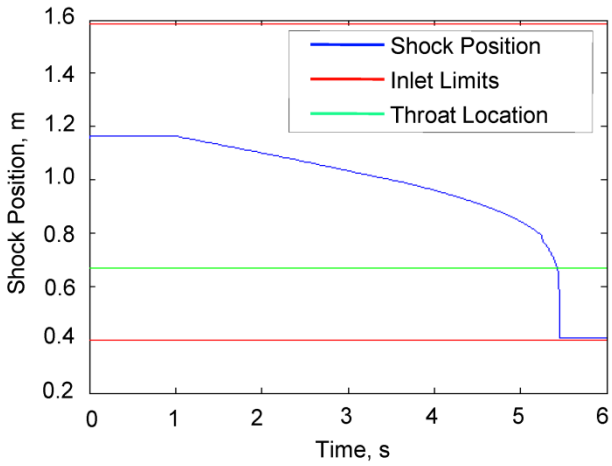

Figure 8. Shock Position as a Function of Time for Increasing Back Pressure.

cowl lip, at 0.4 m, is an artifact due to the CFD cells of the inlet model only extending to the cowl lip. In terms of controls design, this behavior indicates that if a feedback controls design for shock position is based on linear inlet models, the controls design would need to be validated against nonlinear models (such as NOIMA). The reason is that this sensitivity is too significant (i.e., the linear model is too dependent on the location of the shock near the throat), and it would be difficult to duplicate this behavior using linear models.

Besides thrust dynamics for APSE studies, one of the main purposes of the NOIMA model is to also enable feedback controls design[9] to control the shock position in the presence of internal and external disturbances. The purpose of the controls design is to prevent inlet unstarts while maintaining a high pressure recovery (propulsion efficiency). Thus, even though the steady state accuracy of the model was shown to be relatively good compared to LAPIN, the steady state accuracy is not as important as the dynamic accuracy. The reason is that a steady state inaccuracy of a few percent will have a minimum effect on the designed controller gain and the system bandwidth, while a phase delay inaccuracy or uncertainty on the location of poles and zeros can significantly limit the ability to safely design for a high controls bandwidth. This has a direct impact on the control system performance. This importance was recognized when LAPIN was constructed, and it was validated that LAPIN has good dynamic accuracy.

Dynamic analysis was conducted by perturbing freestream flow conditions at discrete frequencies to plot various transfer functions and compare the results against LAPIN. Figure 9 shows a bode plot of the exit pressure with respect to perturbations in the freestream pressure, while the exit Mach number was held constant. This shows that NOIMA compares well to LAPIN in the lower frequency range. At higher frequencies there is some discrepancy in magnitude. However, it was determined that the displayed NOIMA results are more accurate than those generated by applying continuous logarithmic sweeps to LAPIN simulations. The reason is that for NOIMA, discrete frequencies were used, which generally provides for more accuracy. The fact that the phases are right on top of each other is an indication that the dynamics of the two models are essentially the same. With variable step integration, like that used to simulate NOIMA, care must be exercised to also make sure that the maximum time step is sufficiently low so that the frequency sweep runs at a fixed time step. Otherwise, the transfer function estimation will be in error. Figure 10 shows the shock position transfer function with respect to perturbations in the freestream pressure. Again, the results compare well with LAPIN, which also verifies that the NOIMA and LAPIN models adequately model these dynamics. In terms of controls design, bypass door actuators for shock position control have a bandwidth of about 175 Hz, with a typical outer loop shock position control bandwidth correspondingly lower in frequency. Therefore, an accurate inlet dynamic model up to few hundred Hertz frequency should be adequate for feedback controls design.

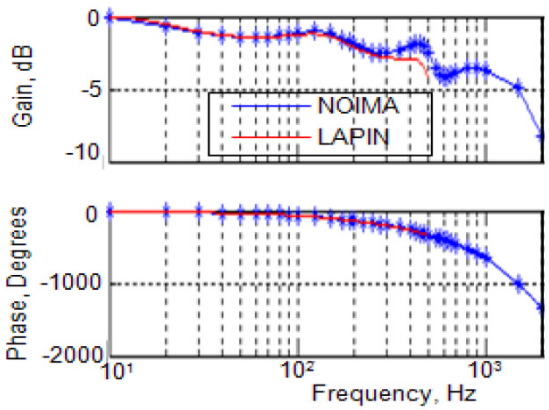

Figure 9. Exit Pressure to Freestream Pressure Transfer Function.

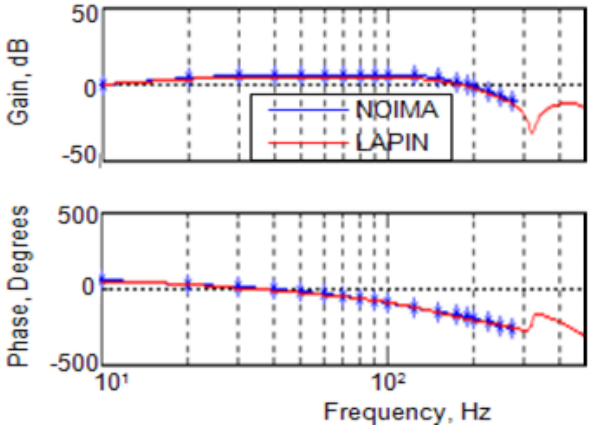

Figure 10. Shock to Freestream Pressure Transfer Function.

IV. Conclusion

A method for modeling mixed compression supersonic inlet dynamics, called NOnlinear Inlet Modeling Assembly (NOIMA), has been developed and verified. The NOIMA approach utilizes a quasi 1 dimensional computational fluid dynamics model for mixed compression inlets incorporating variable geometry, with the external compression portion modeled with compressible flow equations. This type of dynamic model is important for the design of controls to position the normal shock, and for simulating thrust dynamics so that the integrated propulsion and aeroservoelastic systems can be used to study the overall performance for vehicle stability and ride quality. Simulation studies show that this new model compares well with a legacy model in both steady state and frequency response. However, this new model can also be utilized for feedback controls design to position the normal shock, while LAPIN is not suitable for controls design. In addition, this new model runs approximately 3 times faster. Also, given the accuracy of the simulation and that it was developed in the MATLAB/Simulink environment, it can be used as part of an integrated propulsion and aeroservoelastic system models to validate control designs and to study overall propulsion system and vehicle performance. Future work utilizing NOIMA will depend on the inlet configuration that is chosen as a baseline for the NASA Supersonics project. This NOIMA model will be used as a basis to develop models for other types of supersonic inlets such as the external compression or parametric type inlets.

Appendix

Assuming an ideal gas, and inviscid flow with no frictional losses, the gas dynamics associated by applying continuity of mass, momentum, and energy to a flow are as follows.

$$\frac{\partial}{\partial t}\left(\rho_s A\right)+\frac{\partial}{\partial x}\left(\rho_s A v\right)=0 \tag{A1}$$

$$\frac{\partial}{\partial t}\left(\rho_s A v\right)+\frac{\partial}{\partial x}\left(\rho_s A v^2\right)=-A\frac{\partial P_s}{\partial x} \tag{A2}$$

$$\frac{\partial}{\partial t}\left(\rho_s A E_t\right)+\frac{\partial}{\partial x}\left(\rho_s A v H_t\right)=-P_s\frac{\partial A}{\partial t} \tag{A3}$$

The conservation Eqs. (A1) to (A3) can be expressed as a general formulation as

$$\frac{\partial}{\partial t}\left(W_j\right)=-\frac{1}{A}\frac{\partial}{\partial x}\left(AF_j\right)+\frac{S_j}{A} \tag{A4}$$

Since the area of a supersonic inlet can change in time by manipulating its geometry, first it is necessary to take the partial derivatives in Eqs. (A1) to (A3) with respect to area and then reformulate these equations in terms of Eq. (A4). By applying the chain rule to the time derivative of Eq. (A1), and solving for the time derivative of ρ_s, the continuity equation can be expressed as

$$\frac{\partial \rho_s}{\partial t} = -\frac{1}{A}\frac{\partial(\rho_s A v)}{\partial x} - \frac{\rho_s}{A}\frac{\partial A}{\partial t} \tag{A5}$$

Similarly, by applying the chain rule to Eq. (A2) and solving for the time derivative of $\rho_s v$, the momentum equation can be expressed as

$$A\frac{\partial}{\partial t}(\rho_s v) = -\frac{\partial}{\partial x}(\rho_s A v^2) - A\frac{\partial P_s}{\partial x} - \rho_s v\frac{\partial A}{\partial t} \tag{A6}$$

By reversing the chain rule for the term $A\frac{\partial P_s}{\partial x}$ in Eq. (A6), this term becomes $A\frac{\partial P_s}{\partial x} = A\frac{\partial (AP_s)}{\partial x} - P_s\frac{\partial A}{\partial x}$ Substituting this term into Eq. (A6) and through some algebraic manipulation, this equation becomes

$$\frac{\partial}{\partial t}(\rho_s v) = -\frac{1}{A}\frac{\partial}{\partial x}\left[(P_s + \rho_s v^2)A\right] + \frac{1}{A}\left(P_s\frac{\partial A}{\partial x} - \rho_s v\frac{\partial A}{\partial t}\right) \tag{A7}$$

Taking the energy equation, Eq. (A3), and substituting $E_t = c_v T_s + \frac{v^2}{2}$ and $H_t = c_p T_s + \frac{v^2}{2}$, this equation can be expressed as

$$\frac{\partial}{\partial t}\left[\rho_s A\left(c_v T_s + \frac{v^2}{2}\right)\right] + \frac{\partial}{\partial x}\left[\rho_s A v\left(c_p T_s + \frac{v^2}{2}\right)\right] = -P_s\frac{\partial A}{\partial t} \tag{A8}$$

Then by appropriately substituting the equation of state, $P_s = \rho_s R T_s$, into Eq. (A8), this equation can be expressed as

$$\frac{\partial}{\partial t}\left[A\left(\frac{c_v P_s}{R} + \frac{\rho_s v^2}{2}\right)\right] + \frac{\partial}{\partial x}\left[A\left(\frac{c_p P_s v}{R} + \frac{\rho_s v^3}{2}\right)\right] = -P_s\frac{\partial A}{\partial t} \tag{A9}$$

With the definitions of c_v and c_p (i.e., $c_v = \frac{R}{\gamma - 1}, c_p = \frac{\gamma R}{\gamma - 1}$,) substituted into Eq. (A9), this equation becomes

$$\frac{\partial}{\partial t}\left[A\left(\frac{P_s}{\gamma - 1} + \frac{\rho_s v^2}{2}\right)\right] + \frac{\partial}{\partial x}\left[A\left(\frac{\gamma P_s v}{\gamma - 1} + \frac{\rho_s v^3}{2}\right)\right] = -P_s\frac{\partial A}{\partial t} \tag{A10}$$

By applying the chain rule to the first term of Eq. (A10), solving for its time derivative and then by collecting $\frac{\partial A}{\partial t}$ terms on the right side of the equation, this equation becomes

$$\frac{\partial}{\partial t}\left[\left(\frac{P_s}{\gamma - 1} + \frac{\rho_s v^2}{2}\right)\right] = -\frac{1}{A}\frac{\partial}{\partial x}\left[A\left(\frac{\gamma P_s v}{\gamma - 1} + \frac{\rho_s v^3}{2}\right)\right] - \frac{1}{A}\left(\frac{\gamma P_s}{\gamma - 1} + \frac{\rho_s v^2}{2}\right)\frac{\partial A}{\partial t} \tag{A11}$$

Equations (A5), (A7), and (A11) fit the general form of Eq. (A4), with the following definition of its terms

$$W_1 = \rho_s, \qquad F_1 = \rho_s v, \qquad S_1 = -\rho_s \frac{\partial A}{\partial t}$$

$$W_2 = \rho_s v, \qquad F_2 = P_s + \rho_s v^2, \qquad S_2 = P_s \frac{\partial A}{\partial x} - \rho_s v \frac{\partial A}{\partial t}$$

$$W_3 = \left(\frac{P_s}{\gamma - 1} + \frac{\rho_s v^2}{2} \right), \qquad F_3 = \left(\frac{\gamma P_s v}{\gamma - 1} + \frac{\rho_s v^3}{2} \right), \qquad S_3 = -\left(\frac{\gamma P_s}{\gamma - 1} + \frac{\rho_s v^2}{2} \right) \frac{\partial A}{\partial t}$$

Acknowledgments

The authors would like to express their gratitude to the Supersonics Project of the NASA Fundamental Aeronautics Program for supporting this research effort.

References

[1]Lassaux, G.: "High-Fidelity Reduced-Order Aerodynamic Models: Application to Active Control of Engine Inlets," Master's thesis, Dept. of Aeronautics and Astronautics, MIT, Cambridge, MA, June 2002.

[2]Lassaux, G.: Willcox, K.: "Model reduction for active control design using multiple-point Arnoldi methods," AIAA Aerospace Sciences Meeting & Exhibit, Reno, NV, AIAA-2003-616, January 2003.

[3]Willcox, K.: Megretski, A.: "Fourier Series for Accurate, Stable, Reduced-Order Models for Linear CFD Applications," AIAA Computational Fluid Dynamics Conference, Orlando, FL, AIAA-2003-4235, June, 2003.

[4]Chicatelli, A.: Hartley, T. T.: "A Method for Generating Reduced-Order Linear Models of Multidimensional Supersonic Inlets," NASA/CR-1998-207405.

[5]Varner, M.O.: Martindale, W. J.: Phares, K. R.: Kneile, K. R.: Adams, J. C.: "Large Perturbation Flow Field Analysis and Simulation for Supersonic Inlets Final Report," NASA CR 174676, Oct. 1984.

[6]Kopasakis, G.: Connolly, J. W.: Paxson, D. E.: Ma, P.: "Volume Dynamics Propulsion System Modeling for Supersonics Vehicle Research," Journal of Turbomachinery, Vol. 132, October 2010.

[7]Connolly, J.: Kopasakis, G.: Lemon, K.: "Turbofan Volume Dynamics Model for Investigations of Aero-Propulso-Servo-Elastic Effects in a Supersonic Commercial Transport", 46th AIAA/ASME/SAE/ASEE Joint Propulsion Conference and Exhibit, AIAA-2009-4802, August, 2009.

[8]Connolly, J.: Kopasakis, G.: Paxson, D.: Stuber, E.: Woolwine, K.: "Nonlinear Dynamic Modeling and Controls Development for Supersonic Propulsion System Research," 48th AIAA/ASME/SAE/ASEE Joint Propulsion Conference and Exhibit, AIAA 2011-5635, August, 2011

[9]Kopasakis, G.; Connolly, J W.: "Shock Positioning Controls Design for a Supersonic Inlet," AIAA 45th Joint Propulsion Conference, AIAA 2009-5117, Denver, Colorado, 2-5 August, 2009.

[10]Anderson, J. D. Jr.: "Modern Compressible Flow with Historical Perspective," second edition, 1990, McGraw-Hill, Inc.

[11]Chapra, S.; "Applied Numerical Methods, 2nd ed.," McGraw-Hill, New York, 2008, pp. 101, 339, 369-377.